

Galactic properties that favour star cluster formation: a statistical view

Samantha C. Berek,^{1,2*} Marta Reina-Campos,^{1,3,4†} Gwendolyn Eadie^{2,5} and Alison Sills³

¹Equal contribution

²David A. Dunlap Department of Astronomy & Astrophysics, University of Toronto, 50 St. George St., Toronto, ON M5S 3H4, Canada

³Department of Physics & Astronomy, McMaster University, 1280 Main Street West, Hamilton, L8S 4M1, Canada

⁴Canadian Institute for Theoretical Astrophysics (CITA), University of Toronto, 60 St George St, Toronto, M5S 3H8, Canada

⁵Department of Statistical Sciences, University of Toronto, 9th Floor, Ontario Power Building, 700 University Ave, Toronto, ON M5G 1Z5, Canada

Accepted XXX. Received YYY; in original form ZZZ

ABSTRACT

The presence or absence of star clusters in galaxies, and the properties of star cluster populations compared to their host galaxy properties, are important observables for validating models of cluster formation, galaxy formation, and galaxy assembly. In this work, we apply a Bayesian approach to fit two models to data from surveys of young clusters in star forming galaxies. The first model is a logistic regression, which allows us to include galaxies which do not have any young clusters. The second model is a hurdle model, which includes galaxies with zero clusters and also incorporates information about the total mass in the cluster system. We investigate two predictors (star formation rate and total stellar mass in the galaxy) and look at clusters younger than 10 or 100 Myr. We find that in all cases, star formation rate is the better predictor for both the probability of hosting clusters and the total mass in the cluster system. We compare our results to similar models for old globular clusters, and conclude that star cluster formation was more abundant and more efficient at higher redshifts, likely because of the high gas content of galaxies at that time.

Key words: galaxies: star clusters: general – galaxies: evolution – galaxies: formation – stars: formation – methods: statistical

1 INTRODUCTION

Massive star clusters have been used as tracers of galaxy assembly and formation for many decades. In their seminal work, [Searle & Zinn \(1978\)](#) used the metallicities of Milky Way globular clusters to postulate that our Galaxy was formed from the hierarchical merging of smaller (dwarf) galaxies and gas clouds. More recently, orbital information for Milky Way globular clusters derived from Gaia proper motions (e.g. [Gaia Collaboration et al. 2018](#); [Baumgardt et al. 2019](#)) combined with cosmological zoom-in simulations of galaxy formation that include star cluster formation and evolution have confirmed and refined our picture of the assembly of Milky Way-mass galaxies (e.g. [Kruijssen et al. 2019, 2020](#)).

Despite the apparent stochasticity of hierarchical assembly and cluster formation, observations show an extremely tight, linear relationship between the total mass of a globular cluster system and the host galaxy’s dark matter halo mass. [Harris et al. \(2015\)](#) first demonstrated the existence of this relation over five orders of magnitude in stellar mass, and more recent work has confirmed the relation ([Burkert & Forbes 2020](#)) and/or extended it in galaxy system mass (e.g. [Harris et al. 2017](#); [Forbes et al. 2018b](#); [Dornan & Harris 2023](#)).

The extension of this relation to low galaxy mass is difficult for two reasons. One, it is very hard to measure the total mass of dwarf galaxies, including their halo, because the tracers that are available at Milky Way mass and above are not as well-behaved for dwarfs.

The second reason is more statistical – at these masses, the predicted number of old massive cluster per galaxy is less than one, whereas star clusters exist in integer quantities. Within a sample of dwarf galaxies, some galaxies will have a cluster (or two or a handful) while others do not have any old clusters. The lowest mass dwarf galaxies are themselves comparable to the mass of a single star cluster in the Milky Way. It has not been clear how to handle this stochasticity in both the observations and models.

Recent work addresses both of these problems ([Eadie et al. 2022](#); [Berek et al. 2023](#)). Going beyond the galaxy halo mass and linear regressions, they investigated the connection between globular cluster system mass and the stellar mass of the galaxy, which is easily measurable. These studies also explored models that explicitly allow for zero values, thus including in their models dwarf galaxies that do not host clusters.

[Eadie et al. \(2022\)](#) tested a variety of models using a sample of Local Group galaxies, nearby isolated dwarfs, and Virgo cluster galaxies, focusing on old globular clusters ($\tau > 8$ Gyr). They fit a logistic regression to model the probability of the presence or absence of globular clusters, and find that at a galaxy mass of approximately $\log_{10}(M_{\text{star}}/M_{\odot}) > 6.8$, galaxies have a 50 per cent chance of hosting an old stellar cluster. They also tested the use of a hurdle model to incorporate estimates of the population mass for galaxies that do have clusters.

The hurdle model introduced in [Eadie et al. \(2022\)](#) is expanded by [Berek et al. \(2023\)](#). The authors develop the HERBAL model, a hierarchical Bayesian hurdle model that uses the luminosity data directly and incorporates measurement uncertainties via an errors-in-

* E-mail: sam.berek@mail.utoronto.ca

† E-mail: reinacampos@mcmaster.ca

variable approach. The HERBAL model treats the true galaxy masses as parameters and also includes a random effect to account for extra scatter in the stellar mass - globular cluster system mass relation. The HERBAL model was fit to a sample of Local Group galaxies and finds that galaxies of approximately $\log_{10}(M_{\text{star}}/M_{\odot}) = 7.2$ have at least a 50 per cent chance of hosting globular clusters. This information provides some important constraints on the galactic conditions under which massive clusters can form.

Models of cluster formation have been successful in reproducing the linear relationship between galaxy mass and globular cluster system mass for both massive galaxies (e.g. [Boylan-Kolchin 2017](#); [Choksi & Gnedin 2019](#); [El-Badry et al. 2019](#); [Bastian et al. 2020](#)) and for low-mass dwarf galaxies ([Chen & Gnedin 2023](#)). In general, these models either confine themselves to old clusters of 10 Gyr or so (equivalent to Milky Way globular clusters) or simply do not make any age cut. The consensus from these models is that the linear correlation is a hallmark of the combination of many physical processes, including cluster formation and hierarchical galaxy assembly. Cluster formation is inferred to proceed in the same way in both central galaxies and in satellites, with a rate that depends only on local gas or galaxy properties, and galaxy mergers over a Hubble time act mostly to add cluster systems together, with a smaller contribution of merger-driven cluster formation. Cluster disruption can also act to sculpt the present-day distribution of old massive star clusters in galaxies.

Studying old cluster systems, however, means that we are affected by both cluster formation and cluster evolution over most of a Hubble time. Even in dwarf galaxies, clusters are subjected to various processes that will lead to mass loss and possible full cluster disruption, such as stellar evolution, two-body relaxation, and tidal shocks (e.g. [Gnedin & Ostriker 1997](#); [Lamers et al. 2005](#); [Gieles & Baumgardt 2008](#)). However, studying very young cluster populations can provide insight, since they are at most minimally affected by mass loss and evolution ([Webb & Sills 2021](#)). Comparisons between young and old cluster populations, and how those populations depend on their galactic properties, can help distinguish between the cluster formation process and how clusters evolve in low-mass galaxies.

In this paper, we make use of the statistical formalism developed in [Eadie et al. \(2022\)](#); [Berek et al. \(2023\)](#) for old cluster populations in dwarf galaxies, and apply it to young cluster systems from recent surveys of young massive clusters in actively star-forming galaxies. We investigate the relative importance of galaxy mass and present-day star formation rate on the presence or absence of star clusters, and on the total mass in the cluster system. In Section 2, we describe the data and our statistical methods; in Section 3 we present the results of our analysis, and we discuss the implications in Section 4.

2 DATA AND METHODS

2.1 Observational data

We obtain our sample of young star cluster populations in nearby star-forming galaxies from three recently published sources: the ANGST survey¹ ([Cook et al. 2012](#)), the LEGUS survey² ([Cook et al. 2019](#), 2023) and the PHANGS-HST collaboration³ ([Turner et al. 2021](#);

[Whitmore et al. 2021](#); [Deger et al. 2022](#); [Lee et al. 2022](#); [Thilker et al. 2022](#)). When a galaxy is present in two or more catalogues, we take the latest measurement as these tend to be more complete and have more accurate total fluxes. We define two cluster samples with different age ranges, one with objects younger than 10 Myr and the second with objects younger than 100 Myr. Although the first sample might be more contaminated by unbound associations (see fig. 15 in [Brown & Gnedin 2021](#)), it also represents the latest state of star formation in those galaxies. Overall, our sample contains data on 34 star-forming galaxies from the ANGST survey, 23 from the LEGUS survey and 5 from the PHANGS-HST collaboration.

To characterize the young star cluster populations, we note whether galaxies contain young clusters, the number of young clusters per galaxy and the young clusters' total mass in the two age ranges. The ANGST survey already lists these quantities in [Cook et al. \(2012\)](#). For the LEGUS dwarf galaxies, we calculate these properties using the latest cluster catalogues ([Cook et al. 2023](#)). We use the objects classified as class 1 or 2 and with valid masses in the catalogues derived using Padova tracks, Milky Way extinction and the CI-based correction method⁴. We also apply a mass cut that selects clusters more massive than $\log_{10}(m/M_{\odot}) > 3.7$ to have complete samples ([Cook et al. 2023](#)). Lastly, for the galaxies from the PHANGS-HST collaboration⁵, we calculate these quantities using class 1 or 2 objects from the machine learning catalogues. We use these catalogues because they go deeper in magnitude than the human-classified ones.

We use the stellar mass and the star formation rate (SFR) to describe the current state of the star-forming galaxies hosting young star cluster populations. For the galaxies present in the ANGST sample, we use the stellar galaxy masses from [Weisz et al. \(2011\)](#), and the colour-magnitude based SFRs for the last 100 Myr from [Cook et al. \(2012\)](#). The galactic properties of the LEGUS dwarf galaxies are taken from [Cook et al. \(2019\)](#) and [Cook et al. \(2023\)](#). The stellar masses for the LEGUS dwarf galaxies are computed using 3.6 μm maps from *Spitzer* ([Cook et al. 2014](#)), and the SFRs are based on FUV fluxes ([Cook et al. 2023](#)). These SFRs roughly correspond to stellar populations of ages of 1–100 Myr old, and they are within a factor of 2 of the SFR determined from either H_{α} emission or resolved stellar populations ([Cook et al. 2023](#)). Finally, the properties of the PHANGS-HST galaxies are listed in [Leroy et al. \(2021\)](#) and calculated from a variety of sources. The stellar masses are computed from high-quality IRAC 3.6 μm ([Sheth et al. 2010](#)) and WISE1 3.4 μm maps ([Leroy et al. 2019](#)), and the SFRs are a linear combination of GALEX FUV and WISE4 22 μm light.

The final sample is shown in Fig. 1; the top panel shows the binary response variable (whether or not a galaxy has young clusters) as a function of galaxy stellar mass, while the bottom panel shows the continuous response variable (total mass in young clusters) as a function of galaxy stellar mass. The colours of the points (along with a colour bar on the right-hand side of the figure) indicate the SFR. We see that massive ($M_{\text{star}} > 10^9 M_{\odot}$) galaxies always host young star clusters, whereas low-mass ($M_{\text{star}} < 10^7 M_{\odot}$) systems do not. For galaxies with stellar masses between $M_{\text{star}} \sim 10^7\text{--}10^9 M_{\odot}$, the existence of clusters seems stochastic: about half of the galaxies contain young star clusters, and the other half do not. When considering the SFR of the galaxy, galaxies with $\text{SFR} \sim 10^{-2} M_{\odot} \text{ yr}^{-1}$ have a 50 per cent probability of having young clusters. As long observed for the

¹ The ACS Nearby Galaxy Survey Treasury

² The Legacy ExtraGalactic UV Survey - <https://legus.stsci.edu>, [Calzetti et al. \(2015\)](#)

³ Physics at High Angular resolution in Nearby Galaxies - *Hubble Space Telescope* - <https://phangs.stsci.edu>

⁴ We find no correlation between the classification of the clusters and the properties of their galaxy.

⁵ The cluster catalogues are available through the PHANGS homepage at the Mikulski Archive for Space Telescopes with doi:[10.17909/t9-r08f-dq31](https://doi.org/10.17909/t9-r08f-dq31)

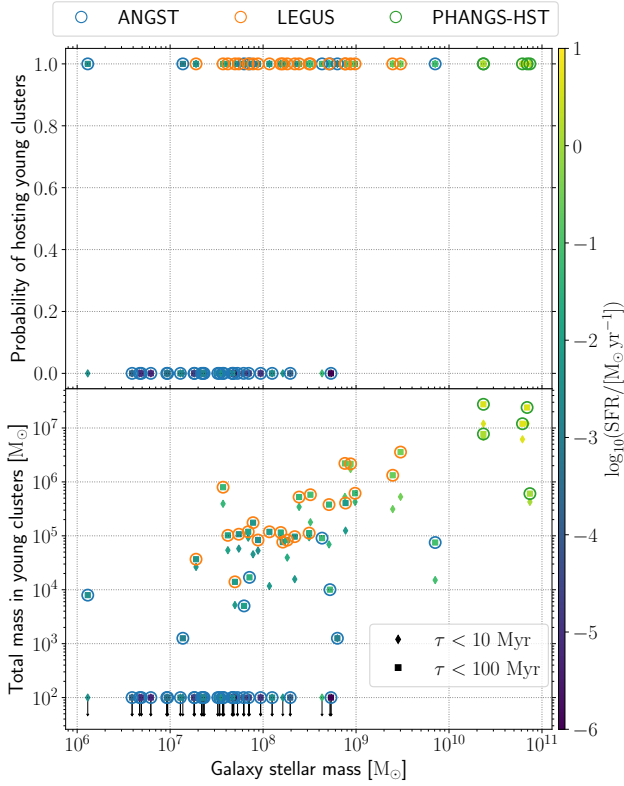


Figure 1. (Top) Flag indicating whether the galaxy hosts young clusters as a function of their galaxy stellar mass. (Bottom) Total mass of young star cluster populations as a function of their host galaxy stellar mass. Galaxies without young clusters are shown as upper limits at $M_{\text{YCS}} = 100 M_{\odot}$. Data points show cluster populations of two different age ranges as indicated in the legend, and are colour-coded by the SFR of their galaxy. The circles around the points indicate to which catalogue the data belongs.

old globular cluster populations (e.g. Peng et al. 2008), the total mass encompassed by the young star cluster population increases towards more massive galaxies. However, the relation shows significant scatter for galaxies with stellar masses between $M_{\text{star}} \sim 10^7\text{--}10^9 M_{\odot}$, suggesting that cluster formation might be a highly stochastic process in these environments.

2.2 Statistical Methods

2.2.1 Logistic Regression

We begin by looking at the relationship between galaxy mass, SFR, and the presence of young star clusters. For this we use logistic regression, which models the probability of a binary success variable - in this case, the presence of young clusters in a galaxy - based on one or multiple predictor variables.

The simplest case of the logistic model has a single predictor variable, the value of which determines the probability of the response variable being 1 or 0. For a single predictor model, the probability of success (i.e., containing at least one cluster) is modeled as

$$p = \{1 + \exp[-(\beta_0 + \beta_1 x)]\}^{-1} \quad (1)$$

where x is the predictor variable and (β_0, β_1) are fit coefficients. We use both \log_{10} SFR and $\log_{10} M_{\text{star}}$ separately as predictor variables in this single-predictor case.

It is straightforward to incorporate multiple predictors into a logistic regression linearly. In a two predictor model, for example, some linear combination of the two predictors (x_1, x_2) (e.g., star formation rate and stellar mass) predicts the presence or absence of young clusters in a galaxy. In the case where x_1 and x_2 are assumed not to interact or depend on one another, the second predictor is linearly added to the first as

$$p = \{1 + \exp[-(\beta_0 + \beta_1 x_1 + \beta_2 x_2)]\}^{-1} \quad (2)$$

If we add interaction, the probability of success becomes

$$p = \{1 + \exp[-(\beta_0 + \beta_1 x_1 + \beta_2 x_2 + \beta_3 x_1 x_2)]\}^{-1} \quad (3)$$

where we now have three fit coefficients $(\beta_0, \beta_1, \beta_2)$.

2.2.2 Lognormal Hurdle Model

The second relationship that we investigate is between our predictor variables \log_{10} SFR and $\log_{10} M_{\text{star}}$ and the mass of young cluster populations. For this we turn to a lognormal hurdle model. Hurdle models have a continuous response variable, in contrast to the binary response from logistic models. Additionally, hurdle models are optimized for data containing a large percentage of zero values, making them well suited for our galaxy sample which contains many galaxies that do not have young clusters.

A lognormal hurdle model is a combination of a logistic model and a linear model (see Berek et al. 2023, for a more detailed description of the hurdle model applied to astronomical data). The logistic model function, as described in the previous section, determines the probability of success (i.e. that a galaxy has young clusters) based on the predictor. Unlike a logistic model, however, the hurdle model describes the non-zero values through a linear regression instead of simply as a binary. The expectation value is a multiplication of these two functions:

$$E[y] = \frac{1}{1 + \exp[-(\beta_0 + \beta_1 x)]} (\gamma_0 + \gamma_1 x), \quad (4)$$

with the first term being the inverse logit function and the second term being a linear regression. The linear β and γ terms can be expanded by adding more coefficients to incorporate multiple predictors in the same way as is demonstrated for the logistic function above.

Uncertainties are incorporated into the hurdle model for both the predictor and response variables via an errors-in-variables model (Berek et al. 2023). For the predictors - \log_{10} SFR and $\log_{10} M_{\text{star}}$ - a normal error distribution is assumed. The measured values of the galaxy properties are considered to be a sample drawn from a normal distribution centered on the true value of the property with a standard deviation equal to the measurement uncertainty:

$$x_{\text{meas}} \sim \mathcal{N}(x_{\text{true}}, \sigma_{\text{meas}}). \quad (5)$$

In the above, x_{true} is the (unknown) true value of the galaxy property, and x_{meas} and σ_{meas} are the measured value and error, respectively.

Uncertainties in the response variable M_{YCS} are built into the linear regression portion of the hurdle model, again assuming a normal distribution of errors. This also assumes that the zero and non-zero populations are entirely separate, as the uncertainties in y only apply to the non-zero portion of the model.

Along with measurement uncertainty, we follow the conclusions of Berek et al. (2023) and add a parameter for unmeasured scatter σ to the overall uncertainty. This scatter term encompasses deviations from linearity and normality, and consists of any intrinsic or otherwise unmeasured sources of uncertainty or scatter in the data.

2.2.3 Bayesian methodology

The logistic and hurdle models were implemented using a Bayesian framework and run using Stan and its RStan interface (Stan Development Team 2022a,b). Stan uses an optimized version of Hamiltonian Monte Carlo (HMC) called a no-U turn sampler (NUTS), which is a gradient-based method of sampling (Hoffman & Gelman 2011; Neal 2011). HMC sampling avoids the random walk behavior of Markov Chain Monte Carlo (MCMC) sampling, which can be prohibitively slow for models with large numbers of parameters. Instead, HMC walks along the peaks of the posterior, exploring only the areas of parameter space that are probable and therefore sampling much more efficiently.

As in Berek et al. (2023) and Eadie et al. (2022), we do not have strong prior knowledge of our parameter distributions, and so we leave our priors relatively broad. For the logistic models using SFR as the predictor variable we use priors of:

$$\beta_0 \sim \mathcal{N}(10, 5)$$

$$\beta_1 \sim \mathcal{N}(3, 5)$$

where $\mathcal{N}(\mu, \sigma)$ are normal distributions of mean μ and standard deviation σ . For the logistic models using stellar mass as a predictor, we use priors of:

$$\beta_0 \sim \mathcal{N}(-13, 5)$$

$$\beta_1 \sim \mathcal{N}(1, 5).$$

The hurdle models require priors for five model parameters: the two logistic β parameters, the two linear γ parameters, and the unmeasured scatter parameter σ . For the models using SFR as a predictor, we use priors of:

$$\beta_0 \sim \mathcal{N}(10, 5)$$

$$\beta_1 \sim \mathcal{N}(3, 5)$$

$$\gamma_0 \sim \mathcal{N}(6, 2)$$

$$\gamma_1 \sim \mathcal{N}(1, 2)$$

$$\sigma \sim \log \mathcal{N}(0, 0.5),$$

and for the models using stellar mass as a predictor we use priors of:

$$\beta_0 \sim \mathcal{N}(-13, 5)$$

$$\beta_1 \sim \mathcal{N}(-1, 5)$$

$$\gamma_0 \sim \mathcal{N}(0, 2)$$

$$\gamma_1 \sim \mathcal{N}(1, 2)$$

$$\sigma \sim \log \mathcal{N}(0, 0.5).$$

2.2.4 Model comparison: leave-one-out cross validation

To compare between versions of our models using different or multiple predictor variables, we use leave-one-out cross validation (LOO-CV; Vehtari et al. 2017). LOO-CV evaluates how good a model is at estimating data not used during the model's training. This allows for numerical comparison of different versions of a model.

The procedure for LOO-CV consists of removing one point from the dataset and then refitting the model with the remaining data. The expected log predictive density (elpd), which is similar to the log likelihood but based on data not used in training the model, is then calculated for the removed point. This gives a measure of how likely the external point is based on the model. This procedure is repeated for each point in the original dataset, and the elpd values are combined to give an overall measure of how good the model is at predicting data. Higher elpd values indicate a more likely model. However,

these values are often multiplied by -2 so that they are on the same scale as other commonly used model comparison methods such as the Akaike information criterion (AIC) and Bayesian information criterion (BIC). We follow this convention, meaning that lower values indicate a better model for our data.

3 RESULTS

We present the best-fit models to describe the probability of a given galaxy to host a young star cluster population, and to predict the total mass in young star clusters. This analysis allows us to investigate which galactic property drives the formation of young star clusters.

3.1 Logistic Regression Models

We assume that the probability of hosting young clusters is driven solely by the global SFR or by the galaxy stellar mass. Under this assumption, we fit logistic regression models with a single predictor to the observational data. We provide the best-fit means in Table 1 and we show the models in Fig. 2.

Coefficients that are significantly different from zero indicate that the corresponding predictor is providing information about whether or not the galaxy has young clusters⁶. Similarly, if a coefficient is not significantly different from zero, then its predictor is not providing information. It is thus important to consider the 95 per cent confidence intervals given on the estimates of each coefficient.

The probability of hosting young ($\tau < 10$ Myr) clusters transitions from 0 to 1 over a wide range in SFRs ($\log_{10}(\text{SFR}/M_{\odot} \text{ yr}^{-1}) = -2.7$ to -1.6) and galaxy stellar masses ($\log_{10}(M_{\text{star}}/M_{\odot}) = 7.4-8.8$). In contrast, the probability of hosting clusters with ages $\tau < 100$ Myr is tightly constrained by the global SFR of the galaxy. Galaxies with star formation activities above $\log_{10}(\text{SFR}/M_{\odot} \text{ yr}^{-1}) > -2.5$ have more than 50 per cent probability of containing clusters younger than $\tau < 100$ Myr. The SFR at which galaxies have a 50 per cent probability of hosting a young cluster is slightly higher for the young age range. In order to form a young star cluster ($\tau < 10$ Myr) after having already formed clusters, galaxies need to sustain a high SFR until the present. However, if their SFR declines after forming a cluster population (e.g. due to the effects of stellar feedback), then no more clusters form.

A similar picture emerges when examining the best-fit means. These are significantly different from zero for the SFR and the stellar mass, thus indicating that both properties provide predictive information. However, the LOO-CV values suggest that the SFR is a better predictor than the stellar mass for both cluster samples.

In addition to the models with single predictors, we also consider whether both the SFR and the stellar mass of a galaxy together drive the probability of hosting young clusters. For this, we model the observational data with a logistic regressions model that has multiple predictors, as well as one with an interaction term. Similar to the models with a single predictor, we have no prior knowledge about the priors. We assume that they are well represented by broad Gaussian distributions, but the best-fit coefficients of both models are very sensitive to these assumptions. Regardless of the priors, however, the $\beta_{M_{\text{star}}}$ coefficients are not significantly different from zero, and so we conclude that there is no information gain in combining the galaxy

⁶ Caution must be placed when interpreting the constant coefficients, as these do not have an intuitive meaning.

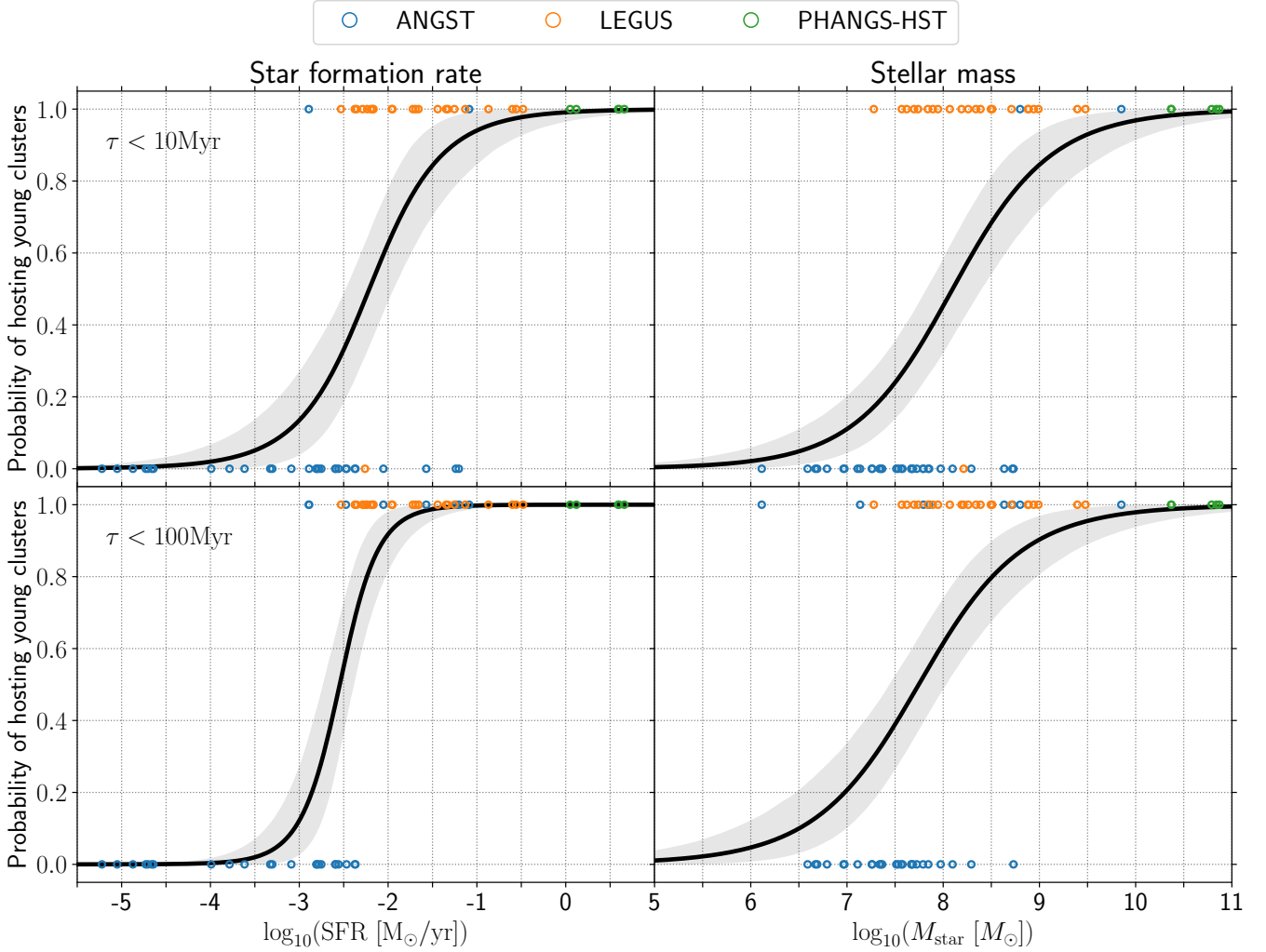


Figure 2. Predicted probability of hosting a young star cluster population from the logistic regression models. These models assume a single predictor: the global star formation rate (*left-hand column*) and the galaxy stellar mass (*right-hand column*). Top and bottom panels correspond to cluster populations younger than 10 Myr and 100 Myr, respectively. Different observational samples correspond to the markers as indicated in the legend. The black solid line with the grey shaded region indicate the mean best-fit and the 90 per cent credible interval, respectively.

Table 1. Best-fit coefficients of logistic regression models predicting the probability of a given galaxy to host a population of young star clusters. The coefficients are means of the posterior distributions. We apply the models to two samples of cluster populations (younger than $\tau < 10$ and $\tau < 100$ Myr). The models assume that either the global SFR or the galaxy stellar mass drive the probability of hosting clusters.

Logistic regression	$\log_{10}(\text{SFR})$			$\log_{10}(M_{\text{star}})$		
	Constant	β_1	LOO-CV	Constant	β_1	LOO-CV
$\tau < 10$ Myr	5.62 (3.07,9.31)	2.54 (1.41,4.13)	51.0 ± 10.1	-15.97 (-22.68,-10.04)	1.97 (1.22,2.81)	58.7 ± 7.2
$\tau < 100$ Myr	12.19 (7.07,18.06)	4.79 (2.75,7.13)	29.7 ± 7.0	-14.56 (-21.30,-8.09)	1.88 (1.06,2.75)	63.4 ± 8.7

Note:

Values in parentheses are 95 per cent credible intervals
 \pm values in LOO-CV column are standard errors

properties⁷. Thus, we just consider models with single predictors for the rest of our analysis.

3.2 Lognormal Hurdle Models

We run an analogous analysis with the lognormal hurdle models to predict the expected mass in young star clusters. This model has the ability to incorporate uncertainties on both the predictor and the response variables. We do not have systematic uncertainties on

⁷ A similar result is obtained for the lognormal hurdle models.

the SFR, galaxy stellar mass, or young cluster masses across our observational sample. Therefore, we assume an uncertainty of a factor of two on the young cluster population masses, and a 30 per cent uncertainty on the galaxy properties. As additional tests, we rerun the analysis for two limiting cases: no measurement uncertainties and inflated uncertainties of a factor of 5 for the cluster population masses and 50 per cent on the galaxy properties. We find that within these bracketing limits, the model is robust to changes in the measurement uncertainties.

We investigate the role of the global SFR or the galaxy stellar mass to separately determine the expected mass of the galaxy's young cluster population. The best-fit coefficients are given in Table 2. As in the logistic regression models, the β_1 coefficients indicate whether the predictor provides information on the probability of galaxies to host young cluster populations. The logistic coefficients of the single predictor hurdle models are similar to those of the logistic regression models, which is to be expected from the fitting algorithm. The γ_1 coefficients correspond to the slope of the relationship between the predictor and the mass of a galaxy's cluster population for those galaxies that have a non-zero cluster population. Thus, these coefficients can be linked to the rate and efficiency of cluster formation.

The corresponding best-fit models are shown in Figure 3. The solid lines indicate the combined expectation value for galaxies with and without young clusters. Thus, these curves cannot be taken as a prediction for the mass of the young cluster population for any single galaxy. Instead, they show the average size of the cluster population for all galaxies of a given stellar mass or SFR, which includes the galaxies that do not have any clusters at all.

The global SFR of a galaxy is a better predictor of the young cluster population mass than its stellar mass. This result holds for both cluster age ranges, with the youngest range having the lowest LOO-CV value.

The SFR has a wide transition region (i.e. the area at which the zero and non-zero populations overlap) for the young age range, $\log_{10}(\text{SFR}/M_{\odot} \text{ yr}^{-1})$ between -3 to -1 , but it narrows for the older age range, $\log_{10}(\text{SFR}/M_{\odot} \text{ yr}^{-1})$ between -3 to -2 . This result is similar to that found in the logistic regression, and it is a consequence of the similarity between the coefficients. In contrast, the expectation models using the galaxy stellar mass as a single predictor show a wide transition for both age bins. Even in the more massive galaxies, the hurdle model predicts a chance of having no clusters. This is seen by the fact that the hurdle fit (solid black line) does not asymptote to the linear fit (dotted line) until a mass of at least $10^{10} M_{\odot}$.

The slopes of the linear portion of the hurdle model contain information on the rate and the efficiency of cluster formation. The slope of the hurdle model using the SFR as a predictor is steeper than that using the galaxy stellar mass. This indicates that cluster population masses increases more rapidly with star formation rate than with galaxy mass. Additionally, the 90 per cent credible region of the SFR model is more compact than that for the stellar mass model, indicating that there is less model uncertainty about the fit. Overall, we find that the global SFR of a galaxy is a better predictor of the expected total mass in young clusters than its present-day stellar mass.

4 SUMMARY AND DISCUSSION

In this paper, we used star cluster and galaxy properties from three different surveys of clusters in star-forming galaxies to investigate the relationship between the presence/absence of young clusters and galactic star formation rate and stellar mass. We used logistic regression and lognormal hurdle models in a Bayesian framework, and

compared different models using the leave-one-out cross validation method. We find that SFR is a better predictor of both the presence of young star clusters and the total mass in young clusters than the present-day stellar mass of the galaxy. This confirms our expectation that the present-day gas properties of a galaxy will drive the formation of stars and clusters simultaneously. These results also provide some insight into the connection between young clusters and their older, more evolved counterparts.

Similar statistical methods have been used to look at old globular cluster systems in galaxies of a wide range of masses. The probability of hosting clusters is represented in Figure 4 for young clusters (black line) from this work, and for globular clusters (purple line) from Eadie et al. (2022), using the logistic regression models with the galaxy stellar mass as the predictor. We find that galaxies host old clusters at lower stellar masses than young, star-forming galaxies; i.e. low-mass galaxies in the past could form and retain clusters, while local galaxies of the same mass are not currently forming clusters.

The linear portion of the expected total cluster population mass from the hurdle model is shown in Figure 5 for young clusters (black line) along with that for old globular clusters (ages greater than 8 Gyr) from Berek et al. (2023). These lines use the present-day galaxy stellar mass as the predictor for the hurdle model. The data used for the Berek et al. (2023) fit includes cluster masses down to $10^2 M_{\odot}$, but the linear portion of that model is not affected by such small systems. Our model for the young clusters has a similar transition region but a shallower slope than the globular cluster model. In other words, older galaxies formed and retained more mass in clusters than galaxies at the present day, and this disparity increases with increasing galaxy mass.

The black arrows in both figures demonstrate the expected evolution of the young cluster system under two main physical processes. First, clusters do not maintain their birth masses over all time, but lose mass due to stellar evolution, two-body relaxation, and tidal shocks (e.g. Gnedin & Ostriker 1997; Lamers et al. 2005; Gieles & Baumgardt 2008). In many cases, clusters will be entirely disrupted. Therefore, both the total mass in clusters and the probability of hosting a cluster should decrease with time at constant galaxy mass. Secondly, the stellar mass in galaxies increases with time (Madau & Dickinson 2014). The total stellar mass of a galaxy at the time that it was forming globular clusters (8-10 Gyr ago) should be less than the present day, unless the star formation rate had a sharp and unexpected truncation to zero immediately after the clusters formed. Therefore, the black line should move to the right in these plots. In both ways of modelling the observational data, Figs. 4 and 5, this expected evolution would move the young population even further from the old globular cluster population, rather than towards it.

These comparisons suggest that it was much easier to form clusters at high redshift. This result is in agreement with many observational and theoretical studies (e.g. Portegies Zwart et al. 2010; Forbes et al. 2018a; Elmegreen 2018; Adamo et al. 2020). If the old cluster population was just the evolved version of the current young cluster population, than the globular cluster fits (purple/red lines) would lie below and/or to the right of the young cluster fits (black lines), as described by the arrows. However, this is not the case. Lower-mass galaxies formed clusters 8-10 Gyr ago, and galaxies of all masses have more mass in old clusters than in young ones. At the same time, our analysis of young cluster populations suggests that there is a stronger connection between current star formation rate (i.e. a current gas property) than galaxy stellar mass. Taken together, we conclude that the gas properties of galaxies at early times were more suitable for cluster formation than at the present day. The cluster formation efficiency (defined as the fraction of stars that formed in

Table 2. Best-fit coefficients of lognormal hurdle models predicting the probability of a given galaxy to host a population of young star clusters, as well as the expected mass of cluster systems for galaxies that do host clusters. The coefficients are the mean of the posteriors. We apply the models to two samples of cluster populations (younger than $\tau < 10$ and $\tau < 100$ Myr). The models assume that either the global SFR or the galaxy stellar mass drive the expected mass of cluster systems.

Hurdle model	β		$\log_{10}(\text{SFR})$		LOO-CV
	β_0	β_1	γ_0	γ_1	
$\tau < 10$ Myr	5.84 (3.09, 9.21)	2.62 (1.42, 4.10)	6.29 (5.97, 6.59)	0.84 (0.65, 1.02)	93.0 ± 14.1
$\tau < 100$ Myr	12.48 (7.06, 18.96)	4.91 (2.75, 7.49)	6.61 (6.25, 6.98)	0.93 (0.72, 1.14)	98.2 ± 13.1
Hurdle model	β		$\log_{10}(M_{\text{star}})$		LOO-CV
	β_0	β_1	γ_0	γ_1	
$\tau < 10$ Myr	-16.17 (-23.03, -9.95)	2.00 (1.23, 2.86)	-0.22 (-2.24, 1.82)	0.62 (0.39, 0.84)	128.0 ± 15.6
$\tau < 100$ Myr	-14.93 (-21.71, -8.71)	1.93 (1.12, 2.80)	-0.60 (-2.51, 1.33)	0.68 (0.46, 0.91)	150.6 ± 16.3

Note: Values in brackets are 95 per cent credible regions
 \pm values in LOO-CV column are standard errors

bound clusters) was higher. This is consistent with our understanding that gas-rich galaxies tend to have higher density gas, resulting in higher star formation rates, higher cluster formation efficiencies, and can form cluster populations that extend to higher initial cluster masses (e.g. Adamo et al. 2020).

The connection between gas properties, young cluster properties, and the subsequent evolution of the cluster system seems fairly straightforward and consistent with our results in this work. However, we are still left with a puzzle – namely, the extremely tight and extremely linear relationship between the globular cluster system mass and the galaxy dark matter halo mass that is observed over many orders of magnitude in halo mass (e.g. Harris et al. 2015; Forbes et al. 2018b). This relationship is not obviously a function just of cluster formation physics or even just of cluster evolution. Galaxy assembly must play an important role. One open observational approach that may shed more light on this is the relationship between cluster populations (young and old) and galaxy dark matter mass at the lowest galaxy masses. Of course, determining the total mass of very low-mass galaxies is extremely challenging and has large uncertainties. But if those masses could be determined at high precision for a large number of galaxies (e.g. Oh et al. 2015), then a hurdle analysis using both young and old clusters with halo mass as the predictor would be critical to learn if the clusters are more dependent on the halo (i.e. galaxy) properties or the star formation rate (i.e. gas properties).

ACKNOWLEDGEMENTS

The authors would like to thank Joshua Speagle for his insight during many conversations about statistical methods and tests. MRC gratefully acknowledges the Canadian Institute for Theoretical Astrophysics (CITA) National Fellowship for partial support; this work was supported by the Natural Sciences and Engineering Research Council of Canada (NSERC). AIS and GME acknowledges funding from the Natural Science and Engineering Research Council of Canada.

Software: This work made use of the following Python packages: Jupyter Notebooks (Kluyver et al. 2016), Numpy (Harris et al. 2020), Pandas (Reback et al. 2020) and Scipy (Jones et al. 2001), and all figures have been produced with the library Matplotlib

(Hunter 2007). The comparison to observational data was done more reliably with the help of the WEBPLOT-DIGITIZER⁸ webtool.

Models were run using the Stan Modeling Language (Stan Development Team 2022a) and R Statistical Software Environment (R Core Team 2022), as well as the following R packages: rstan (Stan Development Team 2022b), plotrix (Lemon 2006), ggplot2 (Wickham 2016), latex2exp (Meschiari 2022), bayesplot (Gabry & Mahr 2022).

DATA AVAILABILITY

All data used in this article is available in the original references and we provide a table with the observational data in Appendix A.

REFERENCES

- Adamo A., et al., 2020, *Space Sci. Rev.*, **216**, 69
 Bastian N., Pfeffer J., Kruijssen J. M. D., Crain R. A., Trujillo-Gomez S., Reina-Campos M., 2020, *MNRAS*, **498**, 1050
 Baumgardt H., Hilker M., Sollima A., Bellini A., 2019, *MNRAS*, **482**, 5138
 Berek S. C., Eadie G. M., Speagle J. S., Harris W. E., 2023, *arXiv e-prints*, p. [arXiv:2306.14945](https://arxiv.org/abs/2306.14945)
 Boylan-Kolchin M., 2017, *MNRAS*, **472**, 3120
 Brown G., Gnedin O. Y., 2021, *MNRAS*, **508**, 5935
 Burkert A., Forbes D. A., 2020, *AJ*, **159**, 56
 Calzetti D., et al., 2015, *AJ*, **149**, 51
 Chen Y., Gnedin O. Y., 2023, *arXiv e-prints*, p. [arXiv:2301.08218](https://arxiv.org/abs/2301.08218)
 Choksi N., Gnedin O. Y., 2019, *MNRAS*, **488**, 5409
 Cook D. O., et al., 2012, *ApJ*, **751**, 100
 Cook D. O., et al., 2014, *MNRAS*, **445**, 899
 Cook D. O., et al., 2019, *MNRAS*, **484**, 4897
 Cook D. O., et al., 2023, *MNRAS*, **519**, 3749
 Deger S., et al., 2022, *MNRAS*, **510**, 32
 Dornan V., Harris W. E., 2023, *arXiv e-prints*, p. [arXiv:2304.11210](https://arxiv.org/abs/2304.11210)
 Eadie G. M., Harris W. E., Springford A., 2022, *ApJ*, **926**, 162
 El-Badry K., Quataert E., Weisz D. R., Choksi N., Boylan-Kolchin M., 2019, *MNRAS*, **482**, 4528
 Elmegreen B. G., 2018, *ApJ*, **869**, 119

⁸ <https://apps.automeris.io/wpd/>

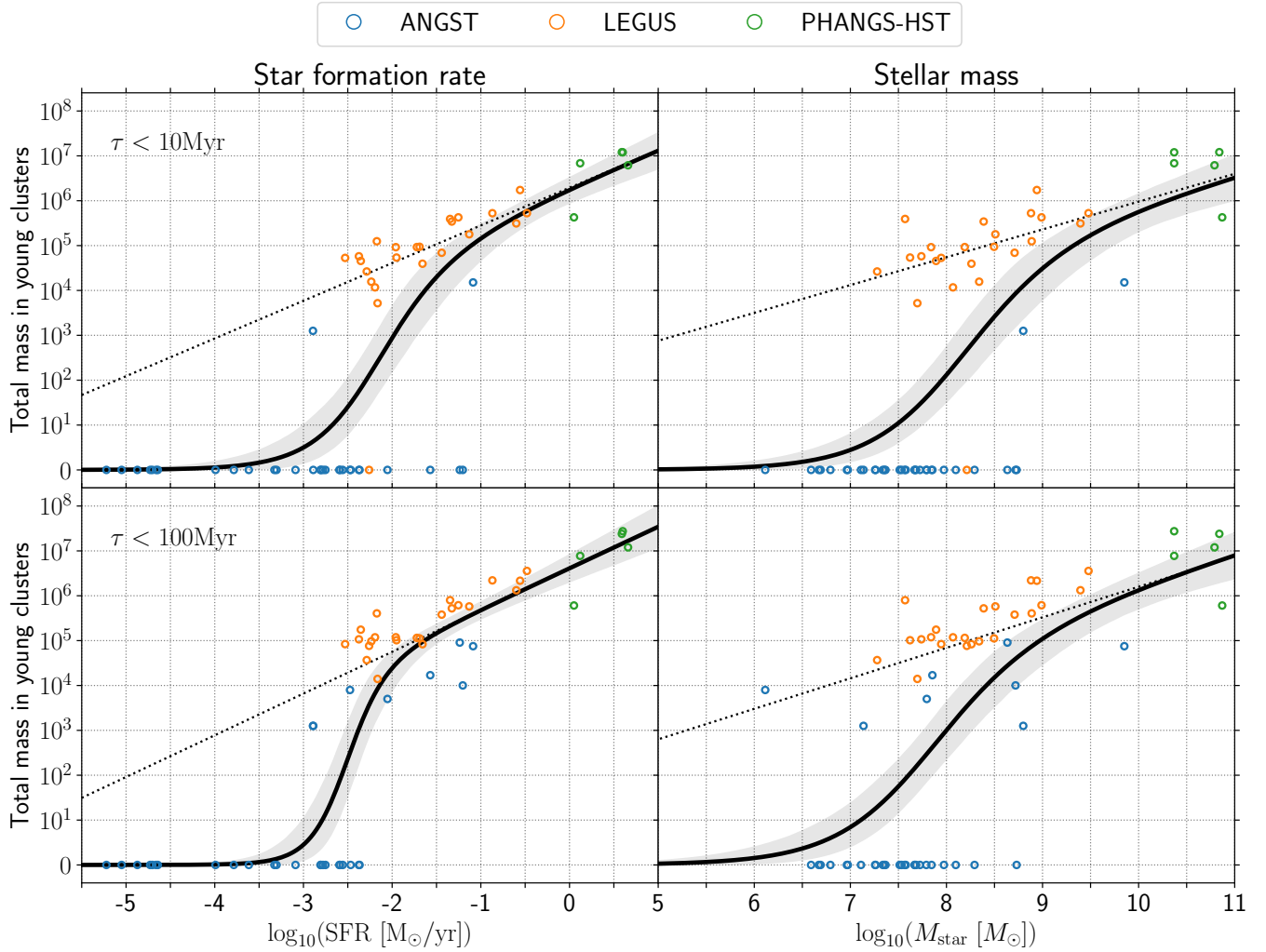


Figure 3. Expected masses of young cluster populations from the hurdle model fits. These models assume a single predictor: the global star formation rate (*left-hand column*) and the galaxy stellar mass (*right-hand column*). Top and bottom panels correspond to cluster populations younger than 10 Myr and 100 Myr, respectively. Different observational samples correspond to the markers as indicated in the legend. In each plot, the black line shows the expectation value of the hurdle model. This is a population level value reflecting the average of the zero and non-zero cluster groups at a given value of the predictor, not an expectation value for a single galaxy. The grey shaded areas are the 90 per cent credible regions, and the dotted lines show just the linear portion of the hurdle model.

Forbes D. A., et al., 2018a, *Proceedings of the Royal Society of London Series A*, 474, 20170616

Forbes D. A., Read J. I., Gieles M., Collins M. L. M., 2018b, *MNRAS*, 481, 5592

Gabry J., Mahr T., 2022, bayesplot: Plotting for Bayesian Models, <https://mc-stan.org/bayesplot/>

Gaia Collaboration et al., 2018, *A&A*, 616, A12

Gieles M., Baumgardt H., 2008, *MNRAS*, 389, L28

Gnedin O. Y., Ostriker J. P., 1997, *ApJ*, 474, 223

Harris W. E., Harris G. L., Hudson M. J., 2015, *ApJ*, 806, 36

Harris W. E., Blakeslee J. P., Harris G. L. H., 2017, *ApJ*, 836, 67

Harris C. R., et al., 2020, *Nature*, 585, 357

Hoffman M. D., Gelman A., 2011, *arXiv e-prints*, p. arXiv:1111.4246

Hunter J. D., 2007, *Computing In Science & Engineering*, 9, 90

Jones E., Oliphant T., Peterson P., et al., 2001, SciPy: Open source scientific tools for Python, <http://www.scipy.org/>

Kluyver T., et al., 2016, Jupyter Notebooks – a publishing format for reproducible computational workflows. pp 87–90, doi:10.3233/978-1-61499-649-1-87

Kruijssen J. M. D., Pfeffer J. L., Reina-Campos M., Crain R. A., Bastian N.,

2019, *MNRAS*, 486, 3180

Kruijssen J. M. D., et al., 2020, *MNRAS*, 498, 2472

Lamers H. J. G. L. M., Gieles M., Bastian N., Baumgardt H., Kharchenko N. V., Portegies Zwart S., 2005, *A&A*, 441, 117

Lee J. C., et al., 2022, *ApJS*, 258, 10

Lemon J., 2006, *R-News*, 6, 8

Leroy A. K., et al., 2019, *ApJS*, 244, 24

Leroy A. K., et al., 2021, *ApJS*, 257, 43

Madau P., Dickinson M., 2014, *ARA&A*, 52, 415

Meschiari S., 2022, latexexp: Use LaTeX Expressions in Plots. <https://CRAN.R-project.org/package=latex2exp>

Neal R. M., 2011, MCMC using Hamiltonian dynamics. Chapman and Hall / CRC press

Oh S.-H., et al., 2015, *AJ*, 149, 180

Peng E. W., et al., 2008, *ApJ*, 681, 197

Portegies Zwart S. F., McMillan S. L. W., Gieles M., 2010, *ARA&A*, 48, 431

R Core Team 2022, R: A Language and Environment for Statistical Computing. R Foundation for Statistical Computing, Vienna, Austria, <https://www.R-project.org/>

Reback J., et al., 2020, pandas-dev/pandas: all versions,

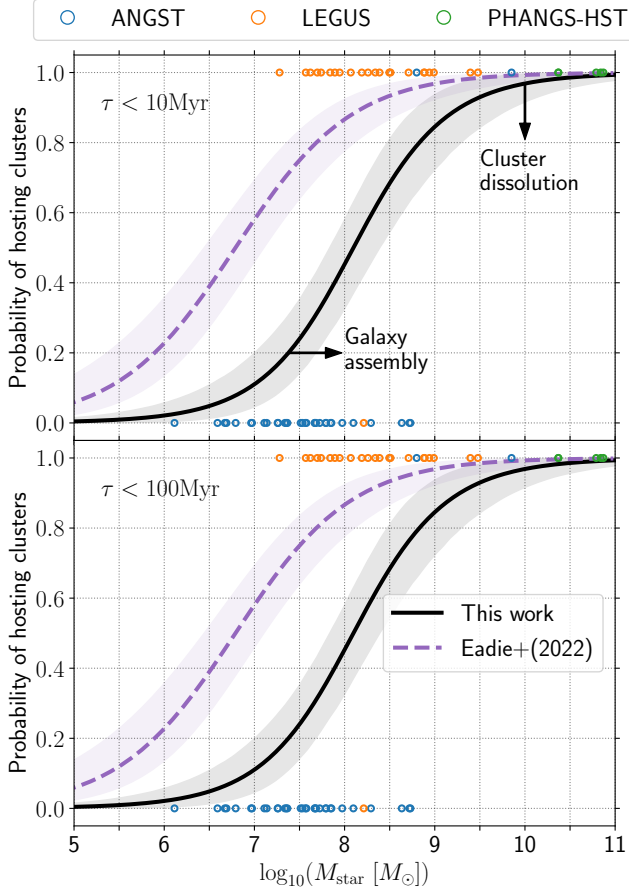


Figure 4. Our logistic regression model for young stellar clusters, using stellar mass as a predictor, is plotted as the black solid line, while the logistic regression for globular clusters from Eadie et al. (2022) is plotted in purple for comparison. The black shaded region corresponds to the 90 per cent credible interval, and the purple shaded region is the 95 per cent confidence interval. Markers correspond to the observational data as indicated in the legend. The black arrows show the expected evolution of the young cluster population under the effects of cluster dissolution (where clusters are lost from the galaxy) and galaxy assembly (where the galaxy gains stellar mass over time).

doi:10.5281/zenodo.3509134, <https://doi.org/10.5281/zenodo.3509134>

Searle L., Zinn R., 1978, *ApJ*, 225, 357

Sheth K., et al., 2010, *PASP*, 122, 1397

Stan Development Team 2022b, RStan: the R interface to Stan, <https://mc-stan.org/>

Stan Development Team 2022a, Stan Modeling Language Users Guide and Reference Manual, Version 2.31, <https://mc-stan.org/>

Thilker D. A., et al., 2022, *MNRAS*, 509, 4094

Turner J. A., et al., 2021, *MNRAS*, 502, 1366

Vehtari A., Gelman A., Gabry J., 2017, *Statistics and Computing*, 27, 1413

Webb J. J., Sills A., 2021, *MNRAS*, 501, 1933

Weisz D. R., et al., 2011, *ApJ*, 739, 5

Whitmore B. C., et al., 2021, *MNRAS*, 506, 5294

Wickham H., 2016, *ggplot2: Elegant Graphics for Data Analysis*. Springer-Verlag New York, <https://ggplot2.tidyverse.org>

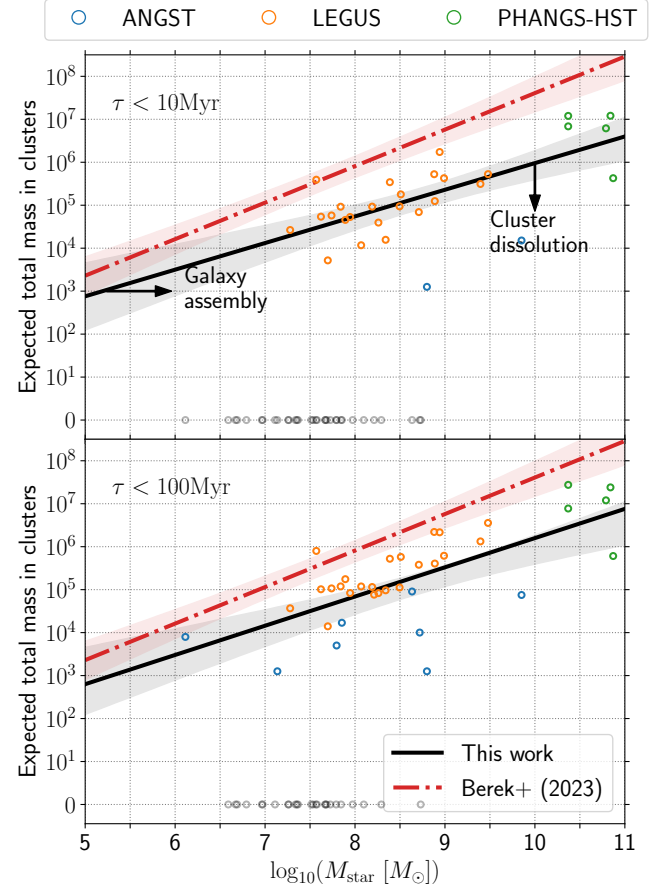


Figure 5. Hurdle model fits with galaxy stellar mass as a predictor. Our model for young clusters is shown as the solid black line, while the hurdle model fit for globular systems (using a hierarchical mass model; Berek et al. 2023) is overplotted as the red dot-dashed line. Shaded regions correspond to the 90 per cent credible interval. The grey shaded regions shows the 90% credible regions. Markers correspond to the observational data as indicated in the legend. Grey markers indicate galaxies without a young star cluster population. The black arrows show the expected evolution of the young cluster population under the effects of cluster dissolution (where clusters are lost from the galaxy) and galaxy assembly (where the galaxy gains stellar mass over time).

APPENDIX A: TABLE OF YOUNG STAR CLUSTERS AND THEIR HOST GALAXIES

We provide in Table A1 the data used in this work. The three observational datasets from which we gather the data are the ANGST survey (Cook et al. 2012), the LEGUS survey (Cook et al. 2019, 2023) and the PHANGS-HST collaboration (Turner et al. 2021; Whitmore et al. 2021; Deger et al. 2022; Lee et al. 2022; Thilker et al. 2022).

This paper has been typeset from a $\text{\TeX}/\text{\LaTeX}$ file prepared by the author.

Table A1. Observational data used in this work. Columns indicate the name of the galaxy, its global star formation rate and stellar mass, as well as flags indicating whether the galaxy contain young star clusters and their total mass for two age ranges, and the observational dataset from which the data was taken (see Sect. 2.1 for more details). Galaxies are ordered by increasing stellar mass.

Galaxy	Galaxy properties		Clusters $\tau < 10$ Myr		Clusters $\tau < 100$ Myr		Sample
	SFR [M_{\odot}/yr]	M_{star} [M_{\odot}]	Flag	M_{YSCs}	Flag	M_{YSCs}	
UGCA292	3.35e-03	1.30e+06	0	–	1	7.94e+03	ANGST
KKR03	2.42e-04	3.90e+06	0	–	0	–	ANGST
HS98-117	8.91e-06	4.70e+06	0	–	0	–	ANGST
ESO540-G030	2.28e-05	4.90e+06	0	–	0	–	ANGST
FM2000-1	6.00e-06	6.20e+06	0	–	0	–	ANGST
KKH98	4.97e-04	9.20e+06	0	–	0	–	ANGST
KDG73	8.14e-04	9.40e+06	0	–	0	–	ANGST
UGC8091	1.77e-03	1.29e+07	0	–	0	–	ANGST
UGC9128	1.29e-03	1.37e+07	0	–	1	1.26e+03	ANGST
UGCA276	1.98e-05	1.81e+07	0	–	0	–	ANGST
BK3N	1.57e-03	1.83e+07	0	–	0	–	ANGST
UGC4459	5.17e-03	1.90e+07	1	2.65e+04	1	3.68e+04	LEGUS
UGC8833	1.56e-03	2.18e+07	0	–	0	–	ANGST
M81dwA	1.66e-03	2.26e+07	0	–	0	–	ANGST
KKH37	4.71e-04	2.32e+07	0	–	0	–	ANGST
UGC8508	2.77e-03	3.26e+07	0	–	0	–	ANGST
ArpsLoop	2.54e-03	3.41e+07	0	–	0	–	ANGST
UGC8651	3.41e-03	3.67e+07	0	–	0	–	ANGST
UGC5340	4.50e-02	3.71e+07	1	3.92e+05	1	7.97e+05	LEGUS
NGC3741	4.22e-03	3.77e+07	0	–	0	–	ANGST
UGCA281	1.12e-02	4.18e+07	1	5.41e+04	1	1.02e+05	LEGUS
UGC5442	1.00e-32	4.66e+07	0	–	0	–	ANGST
UGC8760	4.29e-03	4.69e+07	0	–	0	–	ANGST
UGC5428	1.00e-32	4.83e+07	0	–	0	–	ANGST
UGC5139	6.85e-03	4.98e+07	1	5.20e+03	1	1.40e+04	LEGUS
UGCA133	1.87e-05	5.31e+07	0	–	0	–	ANGST
IC4247	4.22e-03	5.48e+07	1	5.78e+04	1	1.07e+05	LEGUS
KDG61	1.02e-04	6.17e+07	0	–	0	–	ANGST
UGC9240	8.86e-03	6.24e+07	0	–	1	5.01e+03	ANGST
IC559	1.10e-02	6.92e+07	1	9.23e+04	1	1.19e+05	LEGUS
DDO78	2.18e-05	7.00e+07	0	–	0	–	ANGST
UGC5336	2.69e-02	7.14e+07	0	–	1	1.70e+04	ANGST
UGC7242	4.43e-03	7.80e+07	1	4.55e+04	1	1.75e+05	LEGUS
UGC685	2.95e-03	8.82e+07	1	5.32e+04	1	8.36e+04	LEGUS
LEDA166101	1.34e-05	9.41e+07	0	–	0	–	ANGST
NGC5238	6.41e-03	1.17e+08	1	1.17e+04	1	1.19e+05	LEGUS
NGC4163	2.58e-03	1.25e+08	0	–	0	–	ANGST
NGC5477	1.90e-02	1.55e+08	1	9.27e+04	1	1.15e+05	LEGUS
UGC695	5.50e-03	1.63e+08	0	–	1	7.65e+04	LEGUS
ESO486-G021	2.20e-02	1.82e+08	1	3.95e+04	1	8.32e+04	LEGUS
IKN	1.64e-04	1.96e+08	0	–	0	–	ANGST
UGC7408	5.82e-03	2.19e+08	1	1.57e+04	1	9.66e+04	LEGUS
NGC1705	4.71e-02	2.44e+08	1	3.44e+05	1	5.24e+05	LEGUS
UGC4305	2.04e-02	3.13e+08	1	9.40e+04	1	1.12e+05	LEGUS
NGC3274	7.40e-02	3.23e+08	1	1.79e+05	1	5.78e+05	LEGUS
UGC8201	5.79e-02	4.31e+08	0	–	1	9.06e+04	ANGST
NGC3738	3.62e-02	5.12e+08	1	6.92e+04	1	3.80e+05	LEGUS
NGC2366	6.26e-02	5.24e+08	0	–	1	1.00e+04	ANGST
NGC404	1.00e-32	5.37e+08	0	–	0	–	ANGST
UGC5692	1.28e-03	6.30e+08	1	1.26e+03	1	1.26e+03	ANGST
NGC4485	1.35e-01	7.59e+08	1	5.27e+05	1	2.20e+06	LEGUS
NGC4248	6.72e-03	7.71e+08	1	1.25e+05	1	4.05e+05	LEGUS
NGC5253	2.77e-01	8.73e+08	1	1.73e+06	1	2.16e+06	LEGUS
UGC1249	5.58e-02	9.76e+08	1	4.26e+05	1	6.15e+05	LEGUS
NGC4656	2.51e-01	2.48e+09	1	3.13e+05	1	1.33e+06	LEGUS
NGC4449	3.31e-01	3.01e+09	1	5.29e+05	1	3.58e+06	LEGUS
IC2574	8.18e-02	7.10e+09	1	1.51e+04	1	7.51e+04	ANGST
NGC1559	3.98e+00	2.34e+10	1	1.20e+07	1	2.75e+07	PHANGS-HST
NGC3351	1.32e+00	2.34e+10	1	6.85e+06	1	7.74e+06	PHANGS-HST
NGC1566	4.57e+00	6.17e+10	1	6.16e+06	1	1.20e+07	PHANGS-HST
NGC3627	3.89e+00	6.92e+10	1	1.21e+07	1	2.40e+07	PHANGS-HST
NGC1433	1.12e+00	7.41e+10	1	4.26e+05	1	6.06e+05	PHANGS-HST